Mater Renew Sustain Energy (2014) 3:26
DOI 10.1007/s40243-014-0026-5

ORIGINAL PAPER

High-temperature thermoelectric properties of $Cu_{1.97}Ag_{0.03}Se_{1+y}$

Tristan W. Day · Kasper A. Borup · Tiansong Zhang · Fivos Drymiotis · David R. Brown · Xun Shi · Lidong Chen · Bo B. Iversen · G. Jeffrey Snyder

Received: 17 January 2014 / Accepted: 24 February 2014 / Published online: 14 March 2014
© The Author(s) 2014. This article is published with open access at Springerlink.com

Abstract Copper selenide is of recent interest as a high-performance *p*-type thermoelectric material. Adding Ag to copper selenide increases the dimensionless figure-of-merit zT up to 780 K, with $Cu_{1.97}Ag_{0.03}Se$ reaching a zT of 1.0 at 870 K. The increase compared with Cu_2Se can be explained by analyzing the Hall carrier concentration and effective mass. Addition of Ag reduces the carrier concentration to a nearly optimum value at high temperature. If the Hall carrier concentration were to be further reduced to 6.6×10^{20} cm^{-3} at 750 K, the average zT would be substantially improved for waste heat recovery applications.

Keywords Thermoelectrics · Copper selenide · Carrier concentration optimization · $Cu_{1.97}Ag_{0.03}Se_{1+y}$

Introduction

Materials that convert heat directly into electricity, called thermoelectrics, have been used to construct reliable generators of electrical power for spacecraft [1] and, under an applied current, as solid-state cooling devices [2]. Thermoelectric generators and coolers have the advantages of being silent, having no moving parts, and being free from greenhouse and ozone-depleting gases. The maximum efficiency of a thermoelectric material is governed by the figure-of-merit, zT, which is equal to $S^2T\rho^{-1}\kappa^{-1}$, where S is the Seebeck coefficient, T is the absolute temperature, ρ is the electrical resistivity, and κ is the thermal conductivity. Thermoelectric materials in general must have low electrical resistivity, low thermal conductivity, and a controllable carrier concentration.

A new class of high-performance thermoelectric materials is the superionic coinage-metal chalcogenides. Some examples are $Cu_{2-x}Se$ [3], $AgCrSe_2$ [4], $Ag_{2+x}Se$ [5–8], and Ag_2Te [8]. These materials all undergo a structural phase transition above which the metal ions become mobile, which leads to enhanced phonon scattering and consequently low thermal conductivity. This combined with excellent electrical conductivity makes this class of materials promising for use as thermoelectrics.

$Cu_{2-x}Se$ was found to have a zT of 1.5 at 1,000 K [3]. A related compound is $Cu_{1.97}Ag_{0.03}Se_{1+y}$ [9], which was studied from the late 1960s through the late 1970s as a candidate for use in radioisotope thermal generators (RTGs) [10]. The $y = 0$ compound ($Cu_{1.97}Ag_{0.03}Se$), synthesized by 3 M, reached a zT of 1.1 at 870 K [10], which is comparable to the zT of 1.0 at 870 K achieved in $Cu_{1.97}Ag_{0.03}Se$ in this work. Recently, the "overstoichiometric" composition $Cu_{1.98}Ag_{0.2}Se$ was studied and found to reach a maximum zT of 0.52 at 650 K before the onset of bipolar conduction [11]. While $Cu_{1.97}Ag_{0.03}Se_{1+y}$ was tested under RTG conditions in order to evaluate its performance as an energy converter, no attempt was made to analyze its thermoelectric properties in order to optimize its zT. Furthermore, no such analysis has been done for $Cu_{2-x}Se$. Therefore, we seek to analyze these materials together

T. W. Day · F. Drymiotis · D. R. Brown · G. J. Snyder (✉)
Department of Materials Science, California Institute of Technology, Pasadena, CA 91106, USA
e-mail: jsnyder@caltech.edu

K. A. Borup · B. B. Iversen
Department of Chemistry and iNANO, Center for Materials Crystallography, Aarhus University, Aarhus 8000, Denmark

T. Zhang · X. Shi · L. Chen
CAS Key Laboratory of Energy-conversion Materials, Shanghai Institute of Ceramics, Chinese Academy of Sciences, Shanghai 200050, China

to determine the suitability of a single model for describing them and whether they can achieve greater zT values.

The data will be analyzed using an effective mass approach. The premise of this approach is that at a particular temperature, the intricacies of the band structure are reflected by two parameters, the effective mass and the mobility parameter, with the carrier concentration and chemical potential determined from the Hall effect and the Seebeck effect, respectively.

Experimental

Ingots of Cu_2Se, $Cu_{1.98}Se$, $Cu_{1.97}Ag_{0.03}Se$, and $Cu_{1.97}Ag_{0.03}Se_{1.009}$ were formed by melting Cu (shot, 99.9999 % pure, Alfa Aesar, Puratronic), Ag (shot, 99.9999 % pure, Alfa Aesar, Puratronic), and Se (shot, 99.999 % pure, Alfa Aesar, Puratronic) in quartz ampoules evacuated to less than 6×10^{-5} torr. The ampoules were ramped to 1,373 K at 100 K/h, held at that temperature for 12 h, and then quenched. The ingots were ball-milled to form powders, then re-sealed in quartz ampoules, heated at 1,273 K for 5 days, cooled to 973 K, held at that temperature for 3 days and then quenched. The ingots thus obtained were ball-milled again and then hot-pressed at 973 K and 40 MPa for 6 h [12]. The geometric densities of the hot-pressed pellets were greater than 95 % of their theoretical values.

The thermoelectric properties of the samples were measured with custom-built and commercial apparatus. The thermal diffusivity α was measured with a Netzsch LFA 457 laser flash analysis unit. The total thermal conductivity was calculated from $\kappa = \alpha d C_p$, where d is the geometric density, and C_p is the heat capacity. The Seebeck coefficient S was measured with a custom-built device [13] and with an ULVAC ZEM-3. The resistivity ρ and Hall resistance were measured with a custom-built system [14] using van der Pauw geometry and a 2-T magnetic field to determine the Hall carrier concentration $n_H = 1/eR_H$ and the Hall mobility $\mu_H = R_H/\rho$. C_p was measured on a Netzsch 200F3 differential scanning calorimeter from 317 to 913 K.

Powder X-ray diffraction (PXRD) patterns were collected using a Rigaku SmartLab diffractometer equipped with a Cu K_α source, parallel beam optics, and a Rigaku D/tex detector. A hot-pressed pellet of $Cu_{1.97}Ag_{0.03}Se$ was placed under dynamic vacuum on an Anton-Paar DHS-1100 hot stage with an X-ray transparent graphite dome. PXRD patterns were collected at 300 and 420 K and used for phase identification and refinement of the high-temperature phase using the FullProf suite [15]. Diffractograms were recorded every 20 K from 300 to 500 K in the 2Θ range from 10° to 100°. Between these measurements, the sample was heated at 1 K/min, while fast diffractograms were recorded from 24.5° to 54.5° 2Θ and a scan speed of 12°/min.

Results and discussion

Powder X-ray diffraction shows that $Cu_{1.97}Ag_{0.03}Se_{1+y}$ is not single phase (Fig. 1); rather it is composed of $Cu_{2-x}Ag_xSe$, CuAgSe [16], and at least one more unidentified impurity phase, i.e., some of the Ag enters the Cu_2Se matrix and some forms CuAgSe (which has also been evaluated as a thermoelectric material and found to have low zT values) [17]. In $Cu_{1.97}Ag_{0.03}Se$, the CuAgSe phase is observed to dissolve at about 380 K, slightly before the superionic phase transition just above 400 K. At 420 K, all peaks can be indexed and refined in the high-temperature Cu_2Se structure (antifluorite, space group $Fm\bar{3}m$) except for a few, low-intensity peaks from one or more unidentified impurities. The main phase peaks are satisfactorily described by the antifluorite structure when Cu interstitials are incorporated on the octahedral sites and at trigonal planar sites. The atomic positions were stable when refined. The room-temperature Cu_2Se structure is not known but comparison with phase pure Cu_2Se PXRD patterns [18] reveals another set of peaks not belonging to the impurity at high temperatures, CuAgSe, or pure Cu_2Se. These peaks disappear at the phase transition and can hence either be an impurity, which dissolves, or belong to the main phase if this has a slightly different structure than pure Cu_2Se.

In this study, the compositions Cu_2Se, $Cu_{1.98}Se$, $Cu_{1.97}Ag_{0.03}Se$, and $Cu_{1.97}Ag_{0.03}Se_{1.009}$ were synthesized, and data on $Cu_{1.98}Ag_{0.2}Se$ from a recent publication by Ballikaya et al. [11] are included for a more complete analysis.

The thermoelectric properties of a material depend strongly on the Hall carrier concentration, n_H, whose magnitude can vary with temperature and via chemical doping. In the aforementioned materials, n_H can be decreased by substituting Ag for Cu, or increased by adding Se to create Cu^+ vacancies. Each additional Se^{2-} ion is equivalent to 2 Cu^+ vacancies; each Cu^+ vacancy donates one hole to the valence band. Furthermore, previous work on the band gap of Cu_2Se [19] shows that the valence and conduction bands are separated by a band gap much greater than k_BT, so that only one type of carrier is present. The Hall carrier concentration for all samples is shown in Fig. 2a. Above the phase transition, the Hall carrier concentration of $Cu_{1.97}Ag_{0.03}Se_{1.009}$ is greater than that of $Cu_{1.97}Ag_{0.03}Se$ due to the greater deficiency of metal ions. Likewise, the Hall carrier concentration of $Cu_{1.98}Se$ is greater than that of Cu_2Se. This could be because substitution of Ag for Cu alters the native vacancy concentration

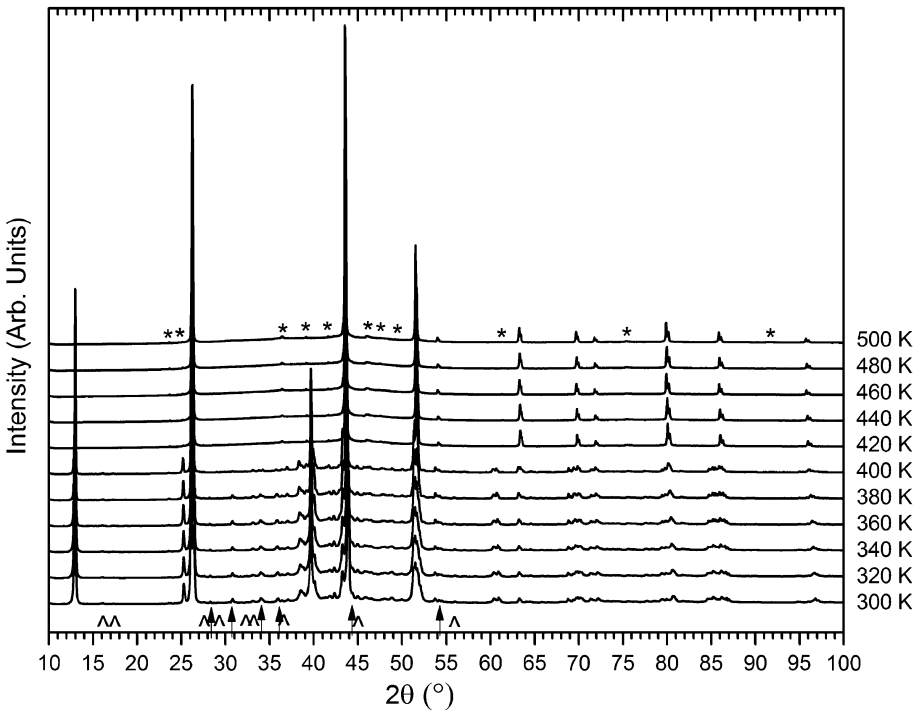

Fig. 1 Temperature resolved PXRD of $Cu_{1.97}Ag_{0.03}Se$ from 300 to 500 K. On the *bottom*, *arrows* mark CuAgSe peaks, while *hat symbol* marks impurities that dissolve at the phase transition. *Asterisk* marks the stable impurity peaks. *Unmarked peaks* on the bottom have corresponding peaks in the low-temperature structure of Cu_2Se

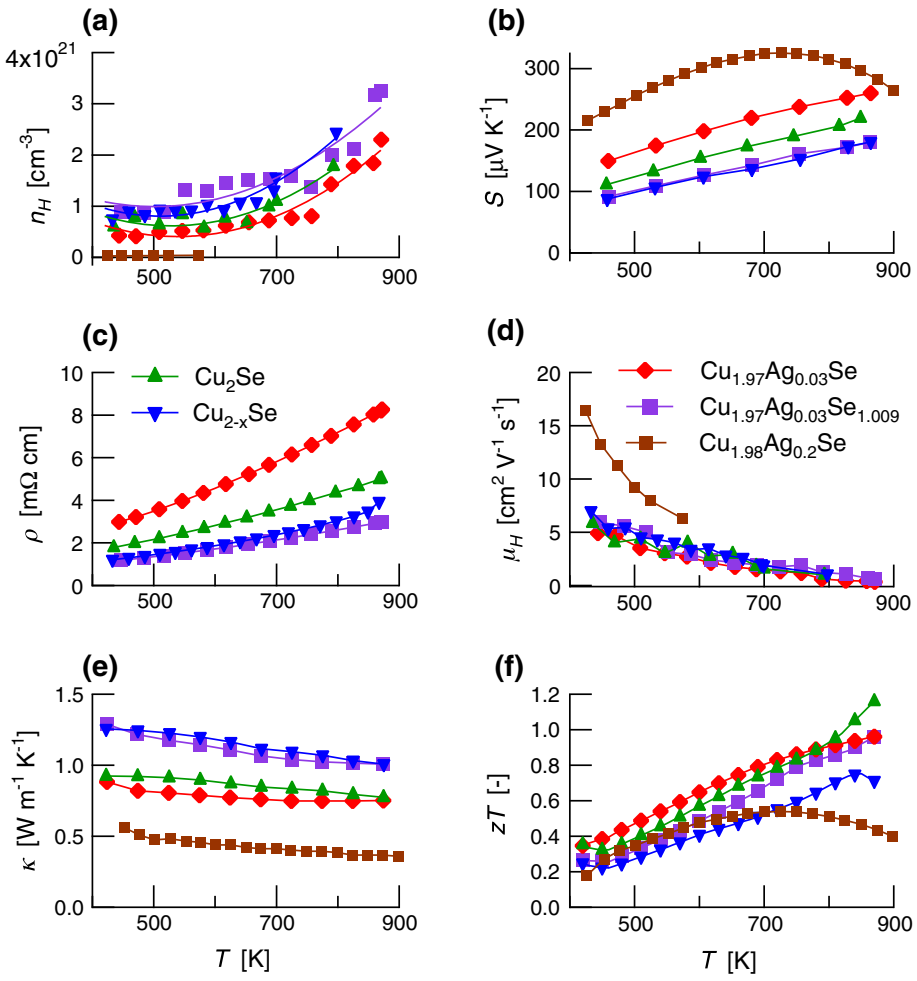

Fig. 2 Transport properties as functions of temperature of $Cu_{2-x}Se$, $Cu_{1.97}Ag_{0.03}Se_{1+y}$ and literature data on $Cu_{1.98}Ag_{0.2}Se$ from Ballikaya et al. [11]. Hall carrier concentration n_H, Seebeck coefficient S, resistivity ρ, Hall mobility μ_H, total thermal conductivity, and figure-of-merit zT are shown in **a**, **b**, **c**, **d**, **e**, and **f**, respectively. The resistivity of $Cu_{1.98}Ag_{0.2}Se$ is not shown because it is several times greater than that of the other compositions. Above the phase transition and up to 780 K, $Cu_{1.97}Ag_{0.03}Se$ achieves higher zT values (**f**) than do Cu_2Se and $Cu_{1.98}Se$ because its Hall carrier concentration is closer to the optimum value (Fig. 3). $Cu_{1.98}Ag_{0.2}Se$ is under-doped compared with both compositions of $Cu_{1.97}Ag_{0.03}Se_{1+y}$, as indicated by its greater Seebeck coefficient (**a**) and lower zT values at all temperatures

of Cu_2Se. The Hall carrier concentration of $Cu_{1.98}Ag_{0.2}Se$ is at least an order of magnitude less ($\sim 10^{19}$ cm^{-3}) than the other compositions ($\sim 10^{20}$–10^{21} cm^{-3}) due to the excess of metal ions [11]. Between 750 and 800 K, the Hall carrier concentrations of $Cu_{2-x}Se$ and $Cu_{1.97}Ag_{0.03}Se_{1+y}$ dramatically increase. The exponential character of this increase seems to indicate bipolar conduction. However, the concomitant decreases in Seebeck and resistivity are not observed. While Hall carrier concentration data for $Cu_{1.98}Ag_{0.2}Se$ were not available above 575 K in Ballikaya et al. [11], the influence of a conduction band separated from the valence band by a band gap of order k_BT is corroborated by the decrease in the Seebeck coefficient of that composition at 725 K, as shown in Fig. 2b.

$Cu_{2-x}Se$ and $Cu_{1.97}Ag_{0.03}Se_{1+y}$ exhibit the steady increase with temperature of the Seebeck coefficient (Fig. 2b) and of the resistivity ρ (Fig. 2c) expected of a single-carrier semiconductor. $Cu_{1.98}Ag_{0.2}Se$ has greater values of S and ρ than do the other samples in the entire temperature range due to its much lower Hall carrier concentration, and it shows a peak in S at about 725 K.

The Hall mobilities, μ_H, of $Cu_{2-x}Se$, $Cu_{1.97}Ag_{0.03}Se_{1+y}$, and $Cu_{1.98}Ag_{0.2}Se$ above the phase transition are low compared with those of other high-performance p-type thermoelectric materials, such as 40–6 cm^2 V^{-1} s^{-1} in Na-doped PbTe between 600 and 750 K, depending on carrier concentration [20]. The Hall mobility scales with T^{-p} [21]. The average value of p taken from the data shown in Fig. 2d and above the phase transition is about 3.1. Values of p between 1 and 1.5 usually indicate that acoustic phonons limit electron mobility in the material [21], while values greater than 1.5 indicate a temperature-dependent effective mass [22].

The thermal conductivity data are shown in Fig. 2e. The sudden increase in κ around the phase transition temperature is due to the sharp peak in C_p [18]. $Cu_{1.98}Ag_{0.2}Se$ has the lowest thermal conductivity values because it has the lowest lattice thermal conductivity, presumably due to disorder caused by the greater amount of Ag, and because it has the lowest carrier concentration of the compositions studied and therefore the lowest electronic thermal conductivity.

The zT data are shown in Fig. 2f. The zT values of $Cu_{2-x}Se$ and $Cu_{1.97}Ag_{0.03}Se_{1+y}$ all increase continuously from the phase transition temperature to the maximum temperature at which they were measured. The $Cu_{1.97}Ag_{0.03}Se$ sample reaches a zT of 1.0 at 870 K. Cu_2Se reaches a zT of 1.16 at 870 K, but between 450 and 780 K has an average zT of 0.59, whereas $Cu_{1.97}Ag_{0.03}Se$ has an average zT of 0.66 in the same temperature range. Above 780 K, the increasing values of ρ in $Cu_{1.97}Ag_{0.03}Se$ and the decreasing values of κ in Cu_2Se mean that Cu_2Se has a greater zT. $Cu_{1.98}Ag_{0.2}Se$ reaches a peak zT of 0.52 at 650 K and then decreases due to bipolar conduction.

To understand why $Cu_{1.97}Ag_{0.03}Se$ achieves a greater zT up to 780 K than do the other samples, we analyze n_H and the effective mass m^*. The carrier mobility in this model is limited by acoustic phonon scattering, and the effective mass is treated as a constant at each temperature. The results of our analysis are shown in Fig. 3 and Table 1.

We estimated the effective mass m^* at 575 K (the highest temperature for which R_H data were available for $Cu_{1.98}Ag_{0.2}Se$) and 750 K (the lowest temperature at which none of the samples exhibit a sharp increase in Hall carrier concentration) by using m^* as a fitting parameter to fit a theoretical curve to S versus n_H data (Fig. 3a). The theoretical dependence of S on the dimensionless Fermi level η is given by Eq. (1). The following equations are valid if the electron mobility is limited by acoustic phonon scattering, as per the discussion of our Hall mobility data above. k_B is Boltzmann's constant, e is the elementary charge, and $F_j(\eta)$ is the Fermi integral of order j, given by Eq. (2). ε is the electronic energy level normalized by k_BT.

$$S = \frac{k_B}{e}\left(\frac{2F_1(\eta)}{F_0(\eta)} - \eta\right) \tag{1}$$

$$F_j(\eta) = \int_0^\infty \frac{\varepsilon^j d\varepsilon}{1 + \exp(\varepsilon - \eta)} \tag{2}$$

η is set by the Hall carrier concentration and the effective mass m^*. The relationship between these variables is given by Eq. (3).

$$n_H = 4\pi\left(\frac{2m^* k_B T}{h^2}\right)^{3/2} F_{1/2}(\eta) \tag{3}$$

At a fixed temperature, we compute η from S for each sample and then use m^* to compute a theoretical n_H that we fit to the n_H data. The effective mass increases with temperature (Table 1), which we predicted based on the Hall mobility data. The same trends of effective mass, Hall carrier concentration, resistivity, and Seebeck coefficient with temperature were observed by Voskanyan et al. [23], though they estimated different values of the effective mass, e.g., 2.2 m_e at 750 K as opposed to 6.2 m_e at 750 K because they used assumed values of n_H instead of calculating them from R_H. Voskanyan et al. proposed a second valence band as a possible cause of the increasing effective mass. While this may explain of the trend of m^* with T, a two-band model is much more complex than a single-band model, requires more assumptions, and does not guarantee a unique solution. Here, we use a single band in this analysis in order to estimate the maximum achievable zT and optimum Hall carrier concentration in this material. We must emphasize that because the

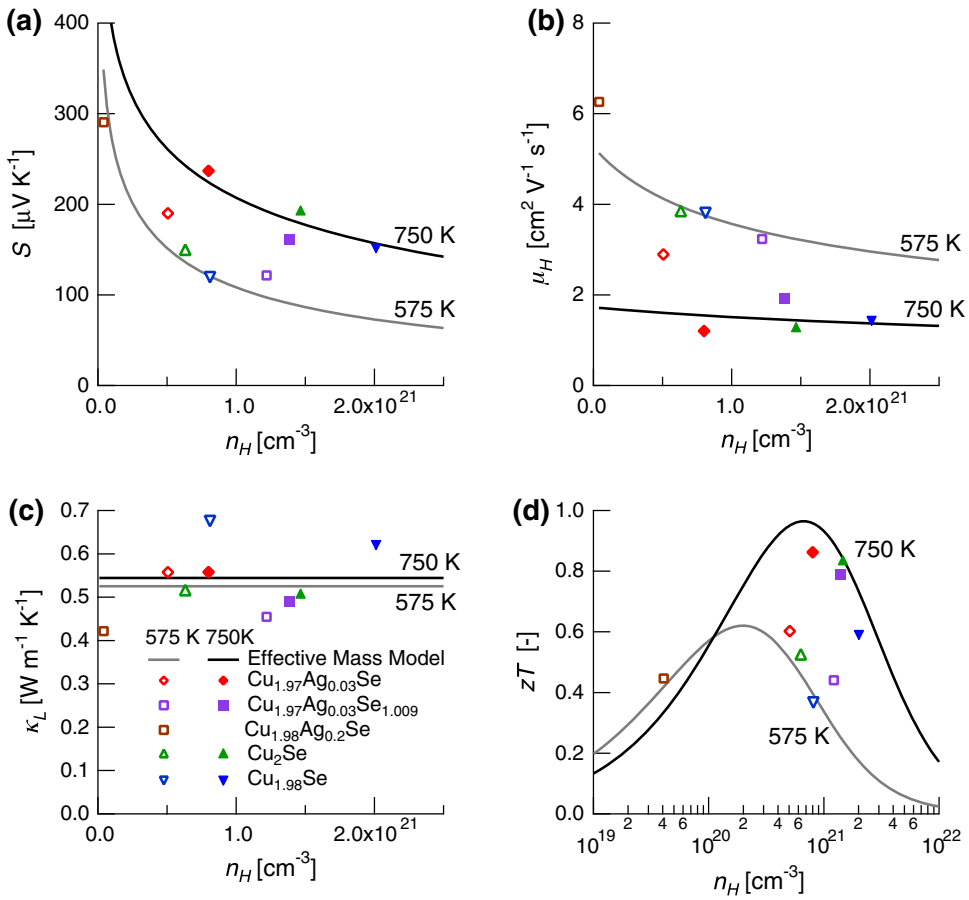

Fig. 3 Analysis of the effective mass and Hall carrier concentration explains and predicts the optimization of $Cu_{1.97}Ag_{0.03}Se$ for thermoelectric use. **a** The Seebeck coefficient as a function of Hall carrier concentration with the effective mass as a fitting parameter. **b** The Hall mobility as a function of Hall carrier concentration with μ_0 as a fitting parameter. The lattice thermal conductivity (**c**) was computed from the resistivity and the Lorenz number *L*. The optimum Hall carrier concentration (**d**) increases with temperature. The Hall carrier concentration of $Cu_{1.97}Ag_{0.03}Se$ also increases with temperature, so it has a Hall carrier concentration close to the optimum value up to 750 K. The *lines* in **c** are average values of κ_L at the indicated temperature

Table 1 Thermoelectric material properties estimated from the effective mass model

	575 K	750 K
m^* (m_e)	3.1	6.2
μ_0 ($cm^2\ V^{-1}\ s^{-1}$)	5.9	1.9
κ_L ($W\ m^{-1}\ K^{-1}$)	0.53	0.54
B (–)	0.28	0.48

effective mass is not constant with temperature, our predictions are valid only at fixed temperatures as a function of Hall carrier concentration.

The estimated values of μ_0 (Table 1) fit to the data shown in Fig. 3b, decrease with temperature, as expected from the raw Hall mobility measurements. The Hall mobility is given by Eq. (4). μ_0 is the mobility of a single electron in the material. The Fermi integral term accounts for energy level degeneracy and scattering. The effective mass m^* and the n_H data are used to compute η, which is then used with the μ_H data to fit μ_0.

$$\mu_H = \mu_0 \frac{F_{-1/2}(\eta)}{2F_0(\eta)} \tag{4}$$

$Cu_{1.97}Ag_{0.03}Se_{1.009}$ has a greater Hall mobility than does $Cu_{1.97}Ag_{0.03}Se$, despite having a greater carrier concentration and more defects.

The thermal conductivity is made up of a lattice contribution κ_L and an electronic contribution κ_E. κ_E is equal to LT/ρ, where *L* is the Lorenz number, given by Eq. (5). We estimated the Lorenz number of each sample at each temperature studied using the previously determined Fermi level η. The Lorenz numbers of the samples were between 1.5×10^{-8} and $1.9 \times 10^{-8}\ V^2\ K^{-2}$ at 575 and 750 K, respectively.

$$L = \left(\frac{k}{e}\right)^2 \frac{3F_0(\eta)F_2(\eta) - 4F_1(\eta)^2}{F_0(\eta)^2} \tag{5}$$

κ_L of each composition is shown in Fig. 3c, along with the average κ_L at each temperature, the values of which are shown in Table 1. κ_L does not change significantly from 575 to 750 K; therefore, the optimization of zT in this materials system will hinge only on the electrical transport properties. The slight increase in κ_L with temperature in Table 1 is due to uncertainty in the calculated κ_E. Taking the estimates for m^*, μ_0, and κ_L, we can calculate a zT versus Hall carrier concentration curve to determine the maximum zT at a given temperature and the optimum Hall

carrier concentration (Fig. 3d). Looking at the zT versus Hall carrier concentration curve for 575 K, it is clear that $Cu_{1.98}Ag_{0.2}Se$ is under-doped, leading to a decrease in zT above 650 K due to bipolar conduction. $Cu_{1.97}Ag_{0.03}Se$ has the Hall carrier concentration closest to the optimum value at every temperature at which we calculated an effective mass, which explains why that composition has the greatest zT of all the compositions included in the analysis.

According to our model, a maximum zT of 1.0 at 750 K is possible in this material system. The dimensionless quality factor B [24–26] (Eq. 6) is a measure of the maximum zT at a given temperature and depends only on material properties and temperature.

$$B = \frac{k_B^{7/2}}{2^{1/2}\pi^{3/2}\hbar^3 e}\frac{\mu_0 (m^*)^{3/2} T^{5/2}}{\kappa_L} \quad (6)$$

The quality factors calculated for this material system increase with temperature (Table 1), meaning the theoretical maximum zT also increases with temperature. According to Fig. 3d, the optimum Hall carrier concentration $n_{H,opt}$ increases with temperature as well, which combined with the increasing trend with temperature of n_H in $Cu_{1.97}Ag_{0.03}Se$ means that that composition has a Hall carrier concentration close to $n_{H,opt}$ at and below 750 K.

Conclusions

Our transport property measurements show that below 780 K $Cu_{1.97}Ag_{0.03}Se_{1+y}$ has superior zT values compared with $Cu_{2-x}Se$ because it has a Hall carrier concentration closer to the optimum value. We have analyzed the Hall carrier concentration and effective mass in these materials and in recently published data on $Cu_{1.98}Ag_{0.2}Se$ for a more complete analysis, and found that these materials together follow the trends expected despite the complexity of the atomic structure and presumed complexity of the electronic structure. This model predicts that a maximum zT of 1.0 at 750 K is possible in this material system.

Each zT versus Hall carrier concentration curve in Fig. 3 indicates that zT of Cu_2Se can be increased simply by reducing the Hall carrier concentration. This means that if Cu_2Se is to be a commercially viable thermoelectric material, the addition of expensive Ag may be unnecessary. Any means of removing charge carriers from the material could improve its thermoelectric properties above the phase transition. Such means could include anion substitution [27, 28] or doping with divalent cations [17]. Furthermore, our analysis is based only on electronic parameters, so separate optimization of the lattice thermal conductivity may improve the zT of this material even further.

Acknowledgments T.W.D. and G.J.S. thank the U.S. Air Force Office of Scientific Research for support. T.W.D. thanks Heng Wang for help with the dimensionless quality factor. T.Z., X.S., and L.C. thank for financial support the National Basic Research Program of China (973-program) under Project No. 2013CB632501 and National Natural Science of Foundation of China (NSFC) under Project No. 51222209. K.A.B. and B.B.I. thank the Danish National Research Foundation (DNRF93).

Open Access This article is distributed under the terms of the Creative Commons Attribution License which permits any use, distribution, and reproduction in any medium, provided the original author(s) and the source are credited.

References

1. LaLonde, A.D., et al.: Lead telluride alloy thermoelectrics. Mater. Today **14**(11), 526–532 (2011)
2. Bell, L.E.: Cooling, heating, generating power, and recovering waste heat with thermoelectric systems. Science **321**, 1457–1461 (2008)
3. Liu, H., et al.: Copper ion liquid-like thermoelectrics. Nat. Mater. **11**(5), 422–425 (2012)
4. Gascoin, F., Maignan, A.: Order-disorder transition in $AgCrSe_2$: a new route to efficient thermoelectrics. Chem. Mater. **23**(10), 2510–2513 (2011)
5. Ferhat, M., Nagao, J.: Thermoelectric and transport properties of beta-Ag_2Se compounds. J. Appl. Phys. **88**(2), 813–816 (2000)
6. Aliev, F., Jafarov, M., Eminova, V.: Thermoelectric figure of merit of Ag_2Se with Ag and Se excess. Atomic Struct. Non-electron. Prop. Semicond. **43**(8), 1013–1015 (2009)
7. Day, T. et al.: Evaluating the Potential for High Thermoelectric Efficiency of Silver Selenide. J. Mater. Chem. C. **1**, 7568–7573 (2012)
8. Miyatani, S.: Ionic conduction in β-Ag$_2$Te and β-Ag$_2$Se. J. Phys. Soc. Jpn. **14**(8), 996–1002 (1959)
9. Hampl, E.F.: U. S. Patent 3,853,632. Minnesota Mining and Manufacturing Company, USA (1974)
10. Brown, D.R., et al.: Chemical stability of $(Ag,Cu)_2Se$: a historical overview. J. Electron. Mater. **42**(7), 2014–2019 (2013)
11. Ballikaya, S. et al.: Thermoelectric properties of Ag-doped Cu_2Se and Cu_2Te. J. Mater. Chem. A. **1**, 12478–12484 (2013)
12. LaLonde, A.D., Ikeda, T., Snyder, G.J.: Rapid consolidation of powdered materials by induction hot pressing. Rev. Sci. Instrum. **82**(2), 025104 (2011)
13. Iwanaga, S., et al.: A high temperature apparatus for measurement of the Seebeck coefficient. Rev. Sci. Instrum. **82**(6), 063905 (2011)
14. Borup, K.A., et al.: Measurement of the electrical resistivity and Hall coefficient at high temperatures. Rev. Sci. Instrum. **83**(12), 123902 (2012)
15. Rodríguez-Carvajal, J.: Recent advances in magnetic-structure determination by neutron powder diffraction. Phys. B **192**(1–2), 55–69 (1993)
16. Miyatani, S.: Electronic and ionic conduction in (AgxCu1-x)2Se. J. Phys. Soc. Jpn. **34**(2), 423–431 (1973)
17. Ishiwata, S., et al.: Extremely high electron mobility in a phonon-glass semimetal. Nat. Mater. **12**(6), 512–517 (2013)
18. Brown, D.R., et al.: Phase transition enhanced thermoelectric figure-of-merit in copper chalcogenides. APL Mater. **1** (2013). Art. No. 052107
19. Sorokin, G.P., Papshev, Y.M., Oush, P.T.: Photoconductivity of Cu_2S, Cu_2Se, and Cu_2Te. Sov. Phys. Solid State **7**(7), 1810–1811 (1966)

20. Pei, Y., et al.: High thermoelectric figure of merit in heavy hole dominated PbTe. Energy Environ. Sci. **4**(6), 2085–2089 (2011)
21. Fistul, V.I.: Heavily Doped Semiconductors. Plenum Press, NY (1969)
22. Ravich, Y.I., Efimova, B.A., Smirnov, I.A.: Semiconducting Lead Chalcogenides. Plenum, New York (1970)
23. Voskanyan, A.A., et al.: Electrical properties of copper selenide. Sov. Phys. Semicond. **12**(11), 1251–1253 (1978)
24. Chasmar, R.P., Stratton, R.: The thermoelectric figure of merit and its relation to thermoelectric generators. J. Electron. Control. **7**, 52–72 (1959)
25. Pei, Y., Wang, H., Snyder, G.J.: Band engineering of thermoelectric materials. Adv. Mater. **24**(46), 6125–6135 (2012)
26. Wang, H., et al.: Material design considerations based on thermoelectric quality factor. In: Koumoto, K., Mori, T. (eds.) Thermoelectric Nanomaterials, pp. 3–32. Springer, Heidelberg (2013)
27. Drymiotis, F., et al.: Enhanced thermoelectric performance in the very low thermal conductivity Ag2Se0.5Te0.5. Appl. Phys. Lett. **103** (2013). Art. No. 143906
28. Mansour, B., El Akkad, F., Hendeya, T.: Electrical and thermoelectric properties of some copper chalcogenides. Phys. Status Solidi A **62**(2), 495–501 (1980)